Sensors and Actuators A 253 (2017) 85–90

Contents lists available at ScienceDirect

Sensors and Actuators A: Physical

journal homepage: www.elsevier.com/locate/sna

Phase interrogation birefringent-refraction sensor for refractive index variation measurements

Ruey-Ching Twu*, Chia-Wei Hsueh

Department of Electro-Optical Engineering, Southern Taiwan University of Science and Technology, No. 1 Nan-Tai Street, Yungkang, Tainan 71005, Taiwan

ARTICLE INFO

Article history:
Received 7 July 2016
Received in revised form 4 November 2016
Accepted 21 November 2016
Available online 22 November 2016

Keywords:
Optical sensor
Phase measurement
Heterodyne interferometer

ABSTRACT

A birefringent-refraction (BR) sensor for measuring refractive indices of liquid solutions based on phase interrogation in a heterodyne interferometer is proposed. We theoretically investigate a comprehensive performance comparison between a surface plasmon resonance (SPR) sensor and the proposed BR sensor in terms of sensitivity and the dynamic range in refractive index measurements. In comparison with a typical SPR sensor, the simulations and experiments show that BR sensors can achieve the same order of sensitivity but with a flexible incident angle and a wide RI range.

1. Introduction

Refractive index (RI) measurements of liquids are important for a variety of applications in industry including the chemical and food processing industry [1–4]. Usually, the RIs of liquid solutions are dependent on the concentrations when mixed with other contents [5]. Moreover, RI monitoring can provide real-time performance analysis for lubricant oil and hydrogen fuel cells [6,7]. In optical metrology, the polarization state of a probe light is changed as well as the RI of the tested liquid by using an optical sensor. Various sensors for obtaining these RI measurements have been developed, such as surface plasmon resonance (SPR) [8–10], total internal reflection (TIR) [11,12], refraction beam displacement [13], and focal point shift [14]. Especially, SPR and TIR sensors have been widely demonstrated in optical bulk or waveguide sensors. In recent years, various fiber-based RI monitoring sensors have been successfully demonstrated by utilizing the SPR, interferometric, and grating coupling principles [15–18].

In an SPR sensor, the amplitude and phase of the reflection *p*-wave (electric-field parallel to the incident plane) are abruptly changed at a resonance angle. Otherwise, the reflection *s*-wave (electric-field perpendicular to the incident plane) is slightly changed. By measuring the RI-dependent reflectance of the probe light, angle or wavelength interrogations are proposed [10,19]. The dip curves are shifted due to the resonance conditions changed by the RI variations. The resolution is dependent on the full width at half maximum (FWHM) of the dip signals. Therefore, multi-layer waveguide structures have been proposed to improve the resolutions [19]. In the phase-interrogation approach, a common-path polarization interferometer and a splitting-path Mach-Zehnder interferometer have demonstrated higher sensitivity due to a step-like measured signal [20,21]. Moreover, the precise control of the incident angle and physical parameters of a metallic film (thickness and complex RI) are essential for attaining high sensitivity measurements [8,9]. To overcome the process's imperfections of gold film, the adjustable probing wavelengths are also critical for maintaining high sensitivity measurement [19,22]. Typically, the phase-interrogation SPR achieves high sensitivity values of 10^4–10^5 after optimizations on the fabrication process of metallic films and experimental setup. However, the dynamic range of RI variations is limited due to the intrinsically nonlinear phase curves. To extend the dynamic range, phase-interrogation combined with the angle-interrogation [8] was conducted to overcome such issues. However, these improvements need more signal process procedures and make the measurement system complex.

In the TIR sensors, the probe light is irradiated onto the interface between the prism and liquid. The critical angle is moved dependent on the RI changes of the liquid tested. The angle can be decided by measuring the corresponding pixel with an abrupt intensity change on the CCD camera [23]. Near the critical angle, a tiny RI change can cause an obvious reflectance change [24]. To remain in good linear operation, the dynamic angle range is limited for high sensitivity. When the incident angle is over the critical angle, the two orthogonally polarized lights will have phase delay modula-

* Corresponding author.
E-mail address: rctwu@stust.edu.tw (R.-C. Twu).

http://dx.doi.org/10.1016/j.sna.2016.11.029
0924-4247/

tion depending on the tested liquid's RI. In the phase-interrogation TIR [12], the incident angle is relaxed, and the impact of intensity noise is reduced in comparison with the intensity-interrogation measurements. In contrast to the SPR transducers, the phase curves of the TIR one are smoother, and the sensitivity is lower but with a wider dynamic range.

A birefringent material has been widely applied for fabrication of wave plates, polarization splitters, and tunable phase retarders [25]. To make a wavelength converter through nonlinear optics, high intensity resistant birefringent crystals, such as MgO-doped lithium niobate (MgO:LN) and potassium titanyl phosphate (KTP), are adopted to generate some useful light sources [26,27]. Therein MgO:LN is a uniaxial birefringent crystal with two different refractive indices.

In this study, we present a new birefringent-refraction (BR) sensor and a common-path heterodyne interferometer for measurements of RI variation. The BR sensor was fabricated by using a MgO:LN plate immersed in the tested liquids. The optical phase delay between two orthogonal polarizations (*p*- and *s*-wave) of the probe light is mainly dependent on the incident angle and the RI variations of the liquid solutions. At a constant incident angle, RI variations can be obtained by measuring the phase signals. Furthermore, the comparison between the SPR and the BR sensors, based on the scheme of phase-interrogation, is theoretically studied. The simulations indicate that the BR sensor has the advantages of a wide dynamic range and flexible incident angle with a really simple structure. To evaluate the capability of the proposed BR sensor, different weight percentages of glucose solutions were prepared to explore the relationship between the phase changes and the RI variation.

2. Sensing principles and simulations

Both structures of SPR and BR sensors are shown in Fig. 1. The typical SPR sensor in Kretschmann configuration consists of a prism, metallic film, and the tested liquid. To make reliable metallic film, a thinner adhesion titanium-film is deposited between the metallic film and the prism. In this simulation, only the single gold film (Au) is adopted to discuss the phase sensitivity and dynamic range in the RI variation measurements.

The reflection coefficients of the *p* and *s* waves can be expressed as [28]:

$$r_q = \frac{r_{gm}^q + r_{ml}^q \cdot \exp(j2k_m d)}{1 + r_{gm}^q \cdot r_{ml}^q \cdot \exp(j2k_m d)} = |r_q| \exp(j\phi_q), \quad (1)$$

$$k_m = \frac{2\pi}{\lambda} \cdot n_g \cdot \cos\theta_i, \quad (2)$$

$$\phi_{SPR} = \phi_p - \phi_s. \quad (3)$$

where q (=p or s) represents the p or s wave; k_m is the wave vector perpendicular to the boundary in the gold film; λ and θ_i are the wavelength and incident angle, respectively; the subscripts g, m and l represent the prism, gold film, and liquid, respectively; and d is the thickness of the gold film. r_{gm} represents the Fresnel reflection coefficient at the interface between the prism and the gold film. r_{ml} represents the Fresnel reflection coefficient at the interface between the metal and the liquid. The RIs of the prism, metal, and liquid are represented by n_g, n_m, and n_l, respectively. The reflection coefficients r_p and r_s are both complex numbers, and ϕ_p and ϕ_s indicate the optical phase delay of the p and s waves due to the reflection at the boundary's surface. The amplitudes of the reflected p and s waves are represented by $|r_p|$ and $|r_s|$, respectively. The phase difference between them, $\phi_{SPR} = \phi_p - \phi_s$, is strongly dependent on n_l and θ_i. The BK7 prism with a refractive index of 1.515, Refractive Index Unit (RIU) and gold film with a permittivity of 12 + i1.26 were used for the simulations [29].

A schematic of the proposed BR sensor is depicted in Fig. 1(b). It is designed by inserting a 1 mm thick MgO:LN plate with a square area (10 mm × 10 mm) in a cubic glass cell. The phase difference between the two orthogonal p and s waves of the probe light is represented by:

$$\phi_{BR} = \frac{2\pi}{\lambda} \cdot t \cdot \left(\sqrt{n_e^2 - n_l^2 \cdot \sin^2\theta_i} - \sqrt{n_o^2 - n_l^2 \cdot \sin^2\theta_i} \right), \quad (4)$$

where t is the thickness of the MgO:LN plate. The refractive indices of extraordinary and ordinary are represented by n_e and n_o (n_e = 2.203 and n_o = 2.286 at 632.8 nm) in the MgO:LN [30]. The s-wave is parallel to the n_e-axis of the MgO:LN plate.

Fig. 2 illustrates the simulations of an SPR sensor for studying the phase variation versus the incident angle (53.5–54.5°) under different gold thicknesses and RIs of solutions. Fig. 2(a)–(c) shows the phase response for gold thicknesses of 40 nm, 45 nm, and 47 nm, respectively. According to the typical phase-interrogation SPR scheme employed with a single probing wavelength, the amount of sensitivity incident angle for matching an SPR condition is dependent on the gold's thickness and the RI of the liquids. As shown in Fig. 2(c), the slope (phase vs. angle) becomes steeper when the thickness and RI approach resonance behavior. The phase curves toward a large incident angle as RI increases. Therefore, the phase is changed as well as the RI variation when the optimized incident angle is decided. By choosing the prompt incident angle, the RI variation can be further extracted based on the phase measurements.

Fig. 3 gives the simulation results of the phase change versus the refractive index for the three gold thicknesses and different incident angles ranging from 53.8 to 54.3°. The angle increases at a rate of 0.05°. When the gold thickness of 40 nm is far away from the resonance condition, as shown in Fig. 3(a), the phase curves have

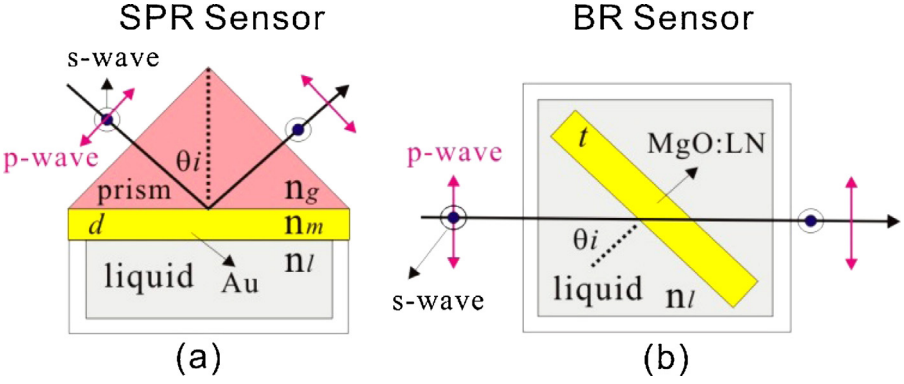

Fig. 1. Device structures for refractive index variation measurement: (a) SPR and (b) BR sensors.

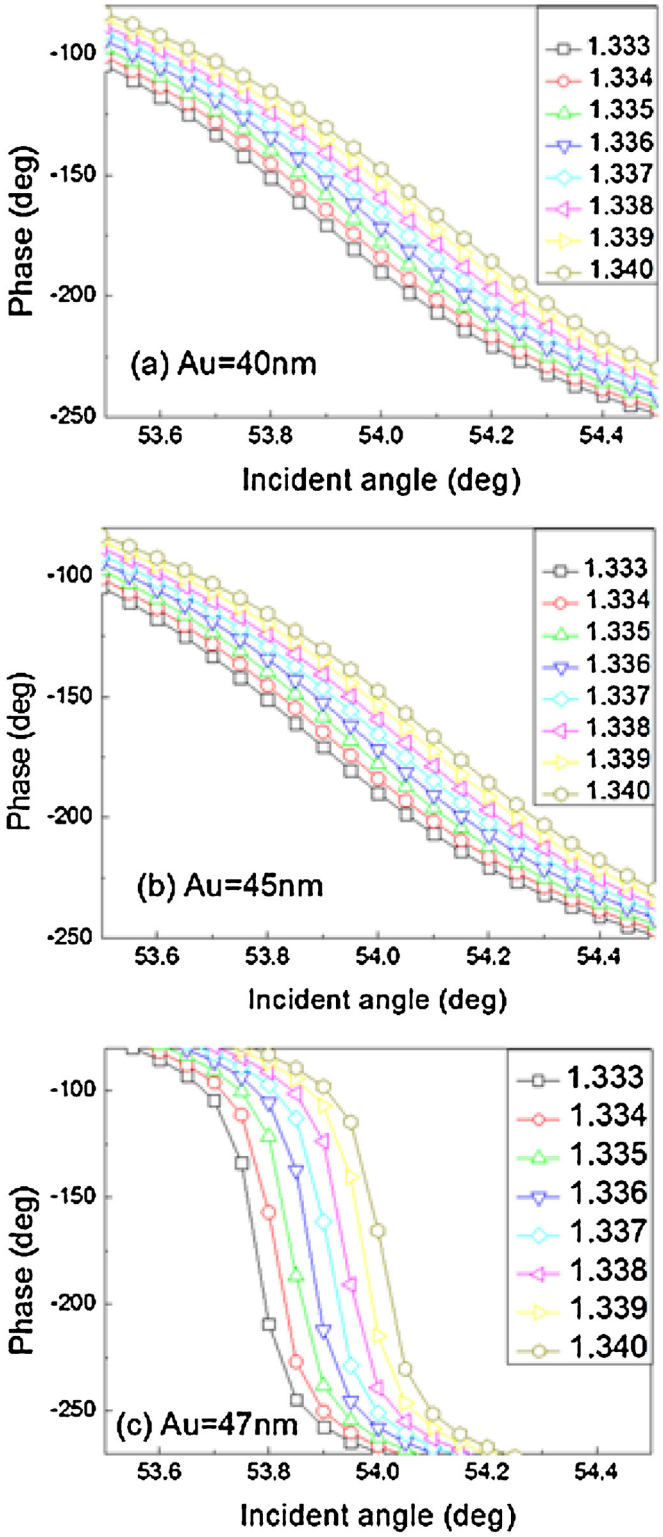

Fig. 2. Phase versus incident angle for different refractive indices of liquid solutions and gold thicknesses: (a) 40 nm, (b) 45 nm, and (c) 47 nm.

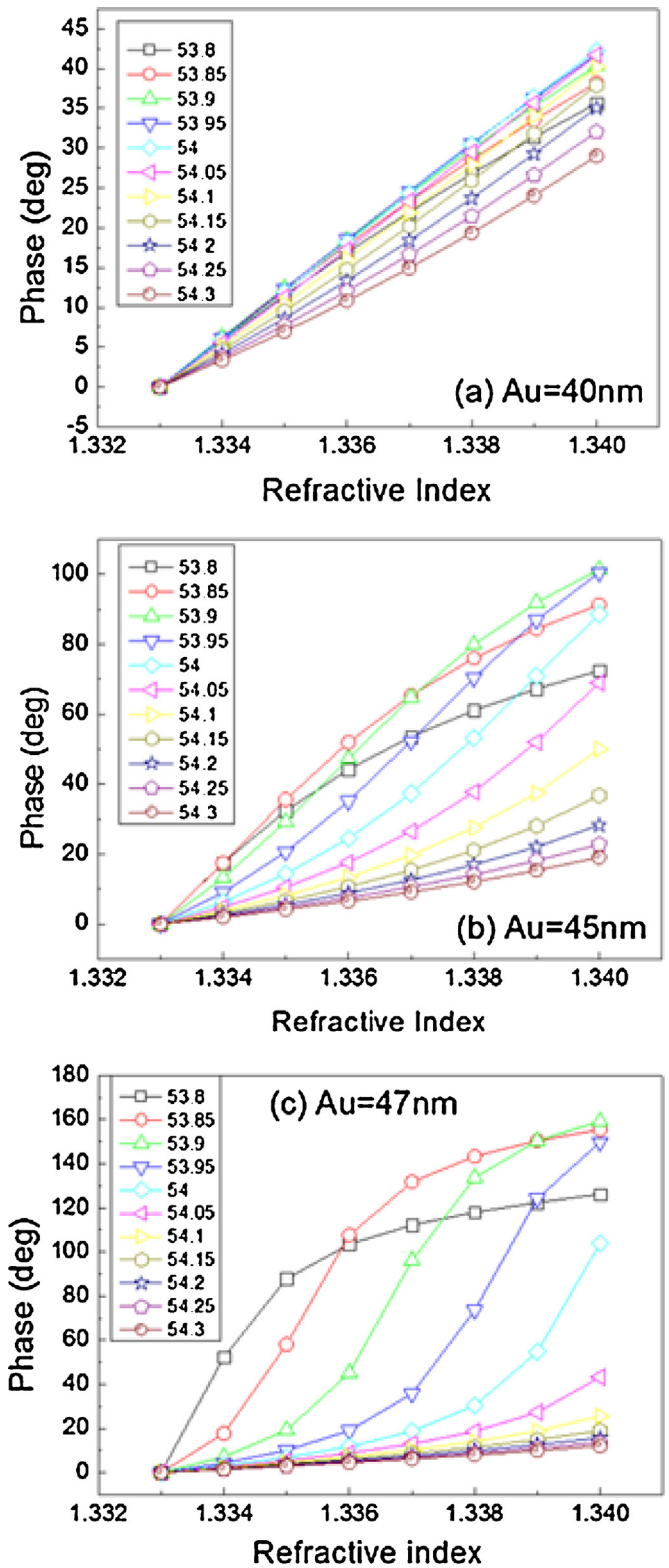

Fig. 3. Phase change versus refractive index of liquid solutions for different incident angles and Au thicknesses: (a) Au = 40 nm, (b) Au = 45 nm, and (c) Au = 47 nm.

a good linearity with the RI within the angle range of 0.5 deg. This means that the setting of the initial incident angle is still easy for experiments. To evaluate the sensing performance, the sensitivity of the RI measurement is defined as a ratio of the phase difference to the RI change. In this case, the sensitivity of the RI measurement is around 4.5×10^3–6×10^3 (deg/RIU). When the gold thickness is increased up to 45 nm, as shown in Fig. 3(b), the best sensitivity is improved up to 1.4×10^4 (deg/RIU) but the linear range of RI measurements is decreased. The measurement phase variations are more sensitive for the optimizations of the incident angle. Fig. 3(c) gives the phase curves at a gold thickness of 47 nm; the sensitivity curves have a nonlinear relationship between the phase and RI. In the case of an incident angle of 53.90 (deg), the best sensitivity is

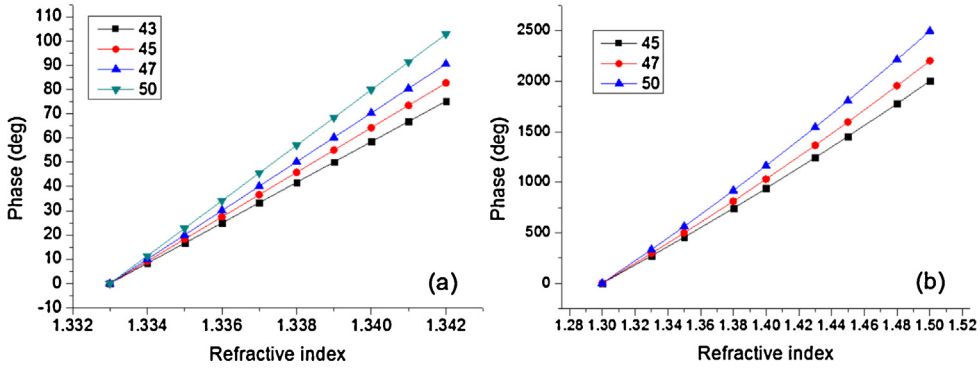

Fig. 4. Phase change versus refractive index for the different incident angles: (a) small RI range and (b) large RI range.

around 4.5×10^4 (deg/RIU) in an RI ranging from 1.336 to 1.338 RIU. The incident angle changed to 53.85 (deg), with the best sensitivity around 4.4×10^4 (deg/RIU) in the RI ranging from 1.334 to 1.336 RIU. The incident angle changed to 53.95 (deg), with the best sensitivity around 4.4×10^4 (deg/RIU) in the RI ranging from 1.337 to 1.339 RIU. The quasi-linear RI regions of the phase curves are deeply dependent on the incident angles. This indicates that the good linearity between the phase and RI has a limited dynamic range at the resonance angle. It is necessary to optimize the gold thickness and the incident angle to obtain good linearity and higher sensitivity. Therefore, the fabrications of gold film have to be well controlled for repeatable measurements.

Fig. 4 shows the relationships between the phase variations and RIs for the proposed BR sensor. In the small RI range (1.333–1.342 RIU) as shown in Fig. 4(a), the values of the average sensitivity are 9.2×10^3, 1.0×10^4, and 1.1×10^4 (deg/RIU) for incident angles 45, 47, and 50 (deg), respectively. In the large RI range (1.3–1.5 RIU), as shown in Fig. 4(b), the values of average sensitivity are 1.0×10^4, 1.1×10^4, and 1.2×10^4 (deg/RIU) for incident angles 45, 47, and 50 (deg), respectively. According to the calculations, the phase curves indicate not only good linearity but also a wide RI range and flexible incident angle. Although the sensitivity of the BR sensor is 4 times smaller than that of the SPR one, as discussed in Fig. 3(c), the linearly dynamic range of the BR sensor (0.2 RIU) is 100 times greater than that of the SPR one (0.002 RIU). In comparison with the SPR-based angular-interrogation scheme for real time monitoring on the lubricant degradation [6], the proposed phase-interrogation BR can effectively provide the linear phase measurements under the wide RI changes at some fixed incident angles (as shown in Fig. 4(b)).

3. Measurement setup and results

The measurement setup for refractive index variation measurements in a heterodyne interferometer is schematically shown in Fig. 5. A He-Ne laser (LS) with a 632.8 nm wavelength is launched through a polarizer (PL) at 45°. The input light is coupled into a lithium niobate Zn-In diffused phase modulator

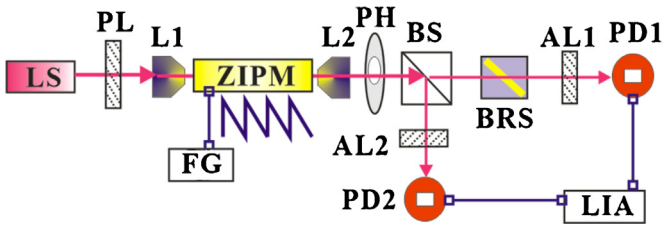

Fig. 5. Experimental setup for refractive index variation measurements in a heterodyne interferometer.

(ZIPM) through an objective lens (L1). The homemade ZIPM is a waveguide-type electro-optic device which was fabricated in an *x*-cut/*z*-propagation substrate. On both sides of the ZI channel waveguide, there are two parallel electrodes 1.8 cm long with a gap width of 12 μm. The detailed fabrication process and the application of ZIPM in the common-path homodyne interferometry have been reported in our previous work [31]. In this experiment, a heterodyne light from the ZIPM can be generated by applying a prompt sawtooth voltage driven from a function generator (FG). The light is then focused by another lens (L2). A pinhole (PH) is used to block the scattering light. The focused light is divided into two different paths after passing through a beam splitter (BS). The transmitted and reflected paths are used as a probe and reference lights, respectively. Therein the probe light passes through the BRS. Next, two analyzers (AL1 and AL2 at 45°), both two sinusoidally interferometric intensity signals, are connected to a lock-in-amplifier (LIA) for measuring the phase delay.

Fig. 6(a) gives the measurements of the applied sawtooth voltage and sinusoidally optical response curve in the ZIPM. The driving voltage and frequency are 5 V and 100 kHz, respectively. Typically, the half-wave voltage of 125 V is necessary for a commercial electro-optic modulator (Model No. 4002, New Focus, Inc.) [32]. The system's phase stability for the ZIPM-based heterodyne interferometer is shown in Fig. 6(b). A phase stability of 0.03 (deg) has been achieved.

We prepared five different solutions with weight percentages 0.625%, 1.25%, 2.5%, 5%, and 10% glucose in deionized water to create liquid RI changes of 8.75×10^{-4}, 1.75×10^{-3}, 3.5×10^{-3}, 7×10^{-3}, and 1.4×10^{-2} RIU, respectively. The solutions were injected into the glass cell by a syringe. The cell was cleaned with deionized water before each experiment. Fig. 7 gives the measured mean phase variation versus RI change at the incident angle of 47 deg. The corresponding concentrations are given for each data point. Actually, the phase values for different glucose concentrations were measured in a period of 50 s (100 data points). Fig. 6(b) gives the phase variations with pure deionized water (0%) in the BRS. To clearly discuss the measurement stability based on a proper error analysis, a root mean square error (RMSE) of the measured data is used to express the phase stability in the measurements. The measured phase variations in the measured 100 data points are taken to calculate the mean values and RMSEs at the different concentrations. The summarized table of the mean values and RMSEs is shown in the inset of Fig. 7. The measurement sensitivity of around 10571 (deg/RIU) is close to the simulated value of 10045 (deg/RIU). The measurement resolution is defined by the ratio of phase stability versus sensitivity. According to the best stability of 0.03 (deg), a measurement resolution of 3×10^{-6} RIU is achievable in the RI range of 1.4×10^{-2} RIU. Moreover, the dynamic RI range can be extended to 0.2 RIU based on the simulations results shown in Fig. 4(b). In comparison with the reported phase-interrogation

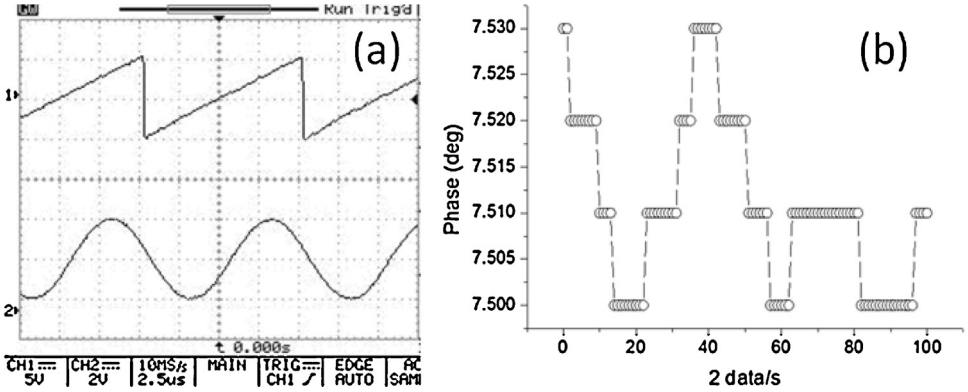

Fig. 6. (a) Measurements of the applied sawtooth voltage and sinusoidally optical response curve, (b) system phase stability for the ZIPM-based heterodyne interferometer.

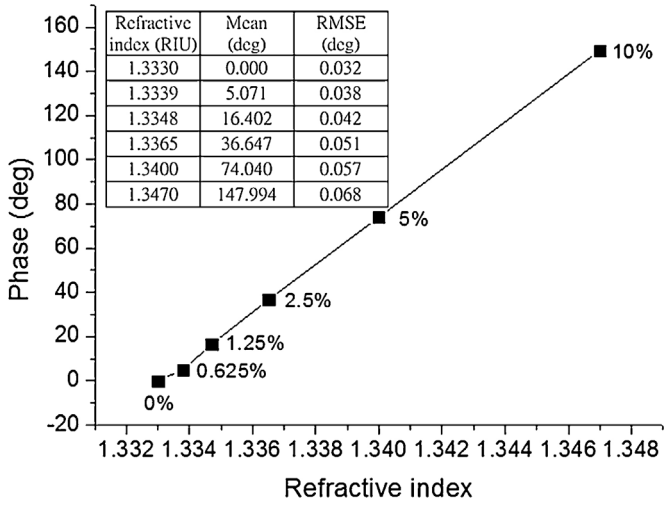

Fig. 7. Phase response for glucose solutions with different concentrations.

SPR sensors [8,9], the extremely high resolution of 2.2×10^{-7} RIU had been achieved while the dynamic range was merely 1.2×10^{-5} RIU at the specific incident angle [8]. The improved wide dynamic range of 6×10^{-2} RIU was possible by combining with the angular-interrogation. However, the arrangements are more complex. In the reference [9], the resolution and dynamic range are 1.5×10^{-6} RIU and 4×10^{-3} RIU, respectively. As a result, the proposed simple BR sensors have the flexibility for sensitivity and dynamic range adjustment.

According the literatures [33,34], a thermal-optic coefficient of isotropic deionized water is -8×10^{-5} [$^{\circ}C^{-1}$], and a thermal-optic birefringent coefficient of LN plate is 3.9×10^{-5} [$^{\circ}C^{-1}$]. The temperature dependent RI changes between the LN and liquid will cause the phase errors during a period of the RI measurements. To avoid the cross-sensitivity between the environmental temperature and RI changes, the thermal stable measurement conditions shall be considered for reducing such issues.

4. Conclusions

In summary, among the various RI measurement schemes [8–14], most of the methods have a tradeoff between resolution and linear dynamic range. It is desirable to have an acceptable resolution with a wide and good linear RI range. In comparison with the TIR and SPR sensors, the sensitivity of the proposed BR sensor is less dependent on the specific incident angles (critical and resonance angle). This means that the flexible incident angle will easily create optical alignment, even by using a manually controlled rotation stage. Unlike the SPR instrument, it needs a fine angle setting for the most sensitivity and repeatable measurements. Moreover, the MgO:LN BR sensor has the properties of chemical resistance. It shall be more robust for repeated measurements in some harsh environments. With the simple structure, high resolution and wide measurement range, the device could have potential applications in the future.

Acknowledgement

This study was supported in part by the Ministry of Science and Technology in Taiwan under grant numbers MOST 104-2221-E-218-027, and MOST 105-2221-E-218-014.

References

[1] M.J. Abuleil, I. Abdulhalim, Birefringence measurement using rotating analyzer approach and quadrature cross points, Appl. Opt. 53 (2014) 2097–2104.
[2] C. Yeh, C. Chow, J. Sung, P. Wu, W. Whang, F. Tseng, Measurement of organic chemical refractive indexes using an optical time-domain reflectometer, Sensors 12 (2012) 481–488.
[3] G.N. Jham, R. Velikova, B.N. Damyavova, S.C. Rabelo, J.C.T. Silva, K.A.P. Souza, V.M.M. Valente, P.R. Cecon, Preparative silver ion TLC/RP-HPLC determination of coffee triacylglycerol molecular species, Food Res. Int. 38 (2005) 121–126.
[4] S. Ariponnammal, A novel method of using refractive index as a tool for finding the adulteration of oils, Res. J. Recent Sci. 1 (2012) 77–79.
[5] H. Sobral, M. Peña-Gomar, Determination of the refractive index of glucose-ethanol-water mixtures using spectroscopic refractometry near the critical angle, Appl. Opt. 54 (2015) 8453–8458.
[6] M. Milanese, A. Ricciardi, M.G. Manera, A. Colombelli, G. Montagna, A. de Risi, R. Rella, Real time oil control by surface plasmon resonance transduction methodology, Sens. Actuators A: Phys. 223 (2015) 97–104.
[7] S. Olyaee, M.S.E. Abadi, S. Hamedi, F. Finizadeh, Refractive index determination in fuel cells using high-resolution laser heterodyne interferometer, Int. J. Hydrogen Energy 36 (2011) 13255–13265.
[8] Y.H. Huang, H.P. Ho, S.Y. Wu, S.K. Kong, W.W. Wong, P. Shum, Phase sensitive SPR sensor for wide dynamic range detection, Opt. Lett. 36 (2011) 4092–4094.
[9] J.Y. Lee, S.K. Tsai, Measurement of refractive index variation of liquids by surface plasmon resonance and wavelength-modulated heterodyne interferometry, Opt. Commun. 284 (2011) 925–929.
[10] S.K. Srivastava, R. Verma, B.D. Gupta, Surface plasmon resonance based fiber optic sensor for the detection of low water content in ethanol, Sens. Actuators B: Chem. 153 (2011) 194–198.
[11] I. Watad, M.A. Jabalee, A. Aizen, I. Abdulhalim, Critical-angle-based sensor with improved figure of merit using dip detection, Opt. Lett. 40 (2015) 4092–4094.
[12] S. Patskovsky, M. Meunier, A.V. Kabashin, Phase-sensitive silicon-based total internal reflection sensor, Opt. Express 15 (2007) 12523–12528.
[13] S. Nemoto, Measurement of the refractive index of liquid using laser beam displacement, Appl. Opt. 31 (1992) 6690–6694.
[14] Q. Li, X. Pu, Measurement of the refractive index of microquantity liquid filled in a capillary and a capillary wall without destruction, Appl. Opt. 52 (2013) 5318–5326.
[15] J. Zhao, S. Cao, C. Liao, Y. Wang, G. Wang, X. Xu, C. Fu, G. Xu, J. Lian, Y. Wang, Surface plasmon resonance refractive sensor based on silver-coated side-polished fiber, Sensor Actuators B: Chem. 230 (2016) 206–211.

[16] Y. Zhao, X. Lia, L. Cai, A highly sensitive Mach–Zehnder interferometric refractive index sensor based on core-offset single mode fiber, Sens. Actuators A: Phys. 223 (2015) 119–124.
[17] A.A. Rifat, G.A. Mahdiraji, Y.M. Sua, R. Ahmed, Y.G. Shee, F.R.M. Adikan, Highly sensitive multi-core flat fiber surface plasmon resonance refractive index sensor, Opt. Express 24 (2016) 2485–2495.
[18] Y.H. Kim, S.J. Park, S.-W. Jeon, S. Ju, C.-S. Park, W.-T. Han, B.H. Lee, Characterization of zinc oxide coated optical fiber long period gratings with improved refractive index sensing properties, Sens. Actuators B: Chem. 223 (2016) 45–51.
[19] F. Bahrami, M. Maisonneuve, M. Meunier, J.S. Aitchison, M. Mojahedi, An improved refractive index sensor based on genetic optimization of plasmon waveguide resonance, Opt. Express 21 (2013) 20863–20872.
[20] C.M. Wu, Z.C. Jian, S.F. Joe, L.B. Chang, High-sensitivity sensor based on surface plasmon resonance and heterodyne interferometry, Sens. Actuators B: Chem. 92 (2003) 133–136.
[21] S.Y. Wu, H.P. Ho, W.C. Law, C. Lin, S.K. Kong, Highly sensitive differential phase-sensitive surface plasmon resonance biosensor based on the Mach-Zehnder configuration, Opt. Lett. 29 (2004) 2378–2380.
[22] A.V. Kabashin, S. Patskovsky, A.N. Grigorenko, Phase and amplitude sensitivities in surface plasmon resonance bio and chemical sensing, Opt. Express 17 (2009) 21191–21204.
[23] S.C. Zilio, A simple method to measure critical angles for high-sensitivity differential refractometry, Opt. Express 20 (2012) 1862–1867.
[24] Augusto Garcıà-Valenzuel, M. Peña-Gomar, C. Garcıà-Segundo, V. Flandes-Aburto, Dynamic reflectometry near the critical angle for high-resolution sensing of the index of refraction, Sens. Actuators B: Chem. 52 (1998) 236–242.
[25] https://www.thorlabs.de/navigation.cfm?guide_id=8.
[26] N.E. Yu, J.H. Ro, M. Cha, S. Kurimura, T. Taira, Broadband quasi-phase-matched second-harmonic generation in MgO-doped periodically poled LiNbO3 at the communications band, Opt. Lett. 27 (2002) 1046–1048.
[27] J. Janousek, S. Johansson, P.T. Lichtenberg, S. Wang, J.L. Mortensen, P. Buchhave, F. Laurell, Efficient all solid-state continuous-wave yellow-orange light source, Opt. Express 13 (2005) 1188–1192.
[28] J. Guo, Z. Zhu, W. Deng, Small-angle measurement based on surface-plasmon resonance and the use of magneto-optical modulation, Appl. Opt. 38 (1999) 6550–6555.
[29] C.M. Wu, M.C. Pao, Sensitivity-tunable optical sensors based on surface plasmon resonance and phase detection, Opt. Express 12 (2004) 3509–3514.
[30] http://www.lasercomponents.com.
[31] R.C. Twu, H.Y. Hong, H.H. Lee, Dual-channel optical phase measurement system for improved precision, Opt. Lett. 33 (2008) 2530–2532.
[32] K.H. Chen, Y.C. Chu, J.H. Chen, Applying the phase difference property of polarization angle for measuring the concentration of solutions, Opt. Lasers Eng. 44 (2012) 251–254.
[33] Y.H. Kim, S.J. Park, S.-W. Jeon, S. Ju, C.-S. Park, W.-T. Han, B.H. Lee, Thermo-optic coefficient measurement of liquids based on simultaneous temperature and refractive index sensing capability of a two-mode fiber interferometric probe, Opt. Express 20 (2012) 23744–23754.
[34] M. Aillerie, M.D. Fontana, F. Abdi, C. Carabatos-Nedelec, N. Theofanous, G. Alexakis, Influence of the temperature-dependent spontaneous birefringence in the electro-optic measurements of LiNbO3, J. Appl. Phys. 65 (1989) 2406–2408.

Biographies

Ruey-Ching Twu received the Ph.D. degree in Graduate Institute of Electro-Optical Engineering (2000) from National Taiwan University, Taiwan. He is currently a professor at Southern Taiwan University of Science and Technology, Department of Electro-Optical Engineering. His research interests include integrated optics, optical metrology systems, and sensors.

Chia-Wei Hsueh received his M.Sc. degree in Department of Electro-Optical Engineering (2012) from Southern Taiwan University of Science and Technology, Taiwan. His research interests include optical waveguide fabrications, and optical sensing applications.